OENO One
vine & wine

DOI: https://doi.org/10.20870/oeno-one.2026.60.2.9833

OPEN ACCESS

ENOLOGY ORIGINAL RESEARCH ARTICLES

Decoding Xinjiang terroir: multimodal element-isotope fingerprints and chemometric data fusion for region-of-origin authentication of wines

Ling Tian[1], Siheng Zheng[2], Henggang Zhou[2], Lu Hai[3,*]

[1] School of Management, Shenzhen Polytechnic University, Shenzhen 518055, China
[2] Guangdong Provincial Key Laboratory of Intelligent Port Security Inspection, Huangpu Customs Technical Center, Guangzhou 510730, China
[3] Division of Chemical Metrology and Analysis Science, National Institute of Metrology, Beijing 100029, China

Article number: 9833

*correspondence:
luhai@nim.ac.cn

Associate editor:
Stamatina Kallithraka

Received:
24 December 2025

Accepted:
22 February 2026

Published:
04 May 2026

This article is published under the **Creative Commons licence** (CC BY 4.0).

Use of all or part of the content of this article must mention the authors, the year of publication, the title, the name of the journal, the volume, the pages and the DOI in compliance with the information given above.

ABSTRACT

Wine origin mislabelling undermines geographical indication (GI) protection and market confidence, calling for robust, data-driven authentication tools adapted to arid continental viticulture. Here, we established an integrated element-isotope fingerprinting and chemometric data-fusion framework to discriminate the region of origin of Xinjiang wines. A total of 473 wines from the 2021 vintage were collected across seven sub-regions (Changji, Hami, Heshuo, Kuerle, Shihezi, Wujiaqu, and Yanqi). Twenty-seven elements were quantified by ICP-MS, and $\delta^{13}C$ (ethanol) and $\delta^{18}O$ (water) were measured by IRMS. After *z*-score standardisation, PCA revealed partial clustering. At the same time, OPLS-DA improved separation and highlighted Li, Na, K, Sr, several trace/transition elements (*e.g.*, Cu, V, Mn, and As) and $\delta^{18}O$ as the main discriminants (VIP > 1). Correlation analysis indicated that climatic aridity, particularly evaporation, temperature and sunshine duration, was a key driver of isotopic enrichment and elemental differentiation. Supervised classification further demonstrated strong predictive performance, with Random Forest achieving the highest accuracy (92 % in 10-fold cross-validation), followed by ANN (88 %), SVM (86 %) and recursive partitioning (79 %). Overall, integrating multi-element and stable-isotope signatures with data-fusion modelling provides a reproducible and accurate approach for terroir differentiation and region-of-origin authentication of Xinjiang wines, supporting GI enforcement in arid viticultural regions.

KEYWORDS: Xinjiang wines, terroir differentiation, elemental-isotopic fingerprints, chemometric modelling, origin authentication, arid viticulture

INTRODUCTION

In the era of globalised wine trade and intensified market competition, authenticity verification and geographical indication (GI) protection have become fundamental pillars for ensuring product credibility and sustaining regional reputation. As wine fraud and origin mislabelling continue to challenge both producers and consumers worldwide, establishing a scientific and traceable origin authentication system has become an urgent priority for the global wine industry (Gao *et al.*, 2025; Kamble *et al.*, 2025). Within this international context, China's emerging wine regions – particularly Xinjiang – are drawing increasing attention for their distinct terroir, extreme climatic conditions, and strategic role in the globalisation of Chinese wine.

Globally, multi-elemental and isotopic fingerprinting has become a mature analytical framework for wine origin traceability and food anti-counterfeiting, with current research increasingly emphasising not only classification accuracy but also marker interpretability and inter-regional comparability (Cellier *et al*., 2021; Epova *et al*., 2019; Erban Kochergina *et al*., 2024; Pesme, 2023; Popîrdă *et al*., 2021; Sun *et al*., 2022). Previous studies have shown that these approaches can produce region-specific provenance signatures rather than only broad group separation. For example, Sr concentration combined with radiogenic δ^{87}Sr has been reported as an effective authenticity marker in regional wine systems, while broader multi-isotope/multi-element strategies have improved PDO-scale discrimination and anti-fraud performance when integrated with chemometric models (Epova *et al*., 2019; Erban Kochergina *et al*., 2024; Popîrdă *et al*., 2021; Sun *et al*., 2022). The isotope systems involved include hydroclimatic tracers such as δ^{18}O (wine water), δ^{13}C (wine ethanol), and deuterium-related parameters (*e.g.*, SNIF-NMR), as well as geogenic/radiogenic tracers such as δ^{87}Sr and, in some regional studies, B and Pb isotope systems (Cellier *et al*., 2021; Epova *et al*., 2019; Erban Kochergina *et al*., 2024; Pesme, 2023). In Europe, isotopic reference infrastructures form the scientific basis for PDO/PGI geographical indication authentication, notably through the EU Wine Databank (JRC framework), which supports official authenticity assessments within regulatory and legal contexts (Crespo-Moncada *et al.,* 2025). At the analytical-method level, internationally recognised wine isotope analysis is aligned with OIV standards, including OIV-MA-AS312-06 (IRMS determination of the δ^{13}C, in wine ethanol) and OIV-MA-AS311-05 (SNIF-NMR determination of deuterium distribution in ethanol, including the parameters (D/H) I, (D/H) II and R). Likewise, in South Africa and Australia, element-isotope models have been incorporated into GI enforcement and export authentication workflows, demonstrating practical value for fraud prevention and label verification in international wine trade (Coetzee *et al.*, 2014; Day & Wilkes, 2021).

Despite these advances, systematic origin-authentication studies in continental arid viticultural systems remain limited, even though such systems are increasingly relevant for climate adaptation research and terroir differentiation under environmental change. Xinjiang, located in the core of Central Asia along the ancient Silk Road, is one of the world's most arid viticultural regions and is characterised by strong continentality, abundant solar radiation, low annual precipitation (< 200 mm), and large diurnal temperature amplitude (> 15 °C) (Guan *et al.*, 2022). These conditions promote high sugar accumulation, balanced acidity, and concentrated aroma expression, while also imposing distinct eco-physiological constraints that shape isotopic and geochemical signatures in grapes and wines (Miao *et al*., 2022; Zhang *et al*., 2021). In contrast to maritime and Mediterranean viticulture, Xinjiang's oasis-desert agroecosystem – sustained largely by glacial-melt irrigation – creates a coupled hydroclimatic-geochemical terroir system in which evaporation intensity, irrigation-water source, soil salinity, and substrate-related geochemistry jointly influence wine typicity (Shi *et al*., 2025; Santesteban *et al*., 2015; van Leeuwen *et al*., 2018; van Leeuwen *et al*., 2020). Under this framework, state-of-the-art recognition of Xinjiang terroir and product wines should be based on coupled isotope-element features, rather than single variables, especially δ^{18}O of wine water (evaporation and water-source signal), δ^{13}C of wine ethanol (vine water status and carbon isotope discrimination), and salinity-/geology-related elemental markers (notably Li, Na, and Sr). To ensure reproducibility and comparability, these features should be evaluated using explicit analytical parameters and validation indices, including VIP values (*e.g.*, VIP > 1) in OPLS-DA, R^2/Q^2 and permutation tests for model validity, and machine-learning performance metrics (accuracy, balanced accuracy, precision, recall, and F1-score). From the perspective of international wine trade and food safety, establishing a scientifically robust origin-authentication system for Xinjiang wines is therefore both strategic and practical; it supports the internationalisation of Chinese-produced wines by aligning domestic GI protection with OIV and EU PDO/PGI-compatible traceability frameworks, while also providing data-based evidence for export authentication, anti-counterfeiting, and terroir-based brand valorisation (Anderson, 2025; Mizik & Balogh, 2022; Yang *et al*., 2022).

Building on this context, the present study develops a sub-regional authentication framework for Xinjiang wines using coupled isotope-element fingerprints, with emphasis on marker interpretability and explicit evaluation parameters. We analysed 473 wines from seven Xinjiang sub-regions using multi-element profiling and stable isotopes (δ^{13}C of wine ethanol and δ^{18}O of wine water), and evaluated discrimination through PCA, OPLS-DA, and machine-learning models (RF, ANN, SVM, and R-Part). The parameters assessed include elemental concentrations, isotope ratios, climatic covariates (temperature, precipitation, sunshine duration, and evaporation), OPLS-DA statistics (R^2X, R^2Y, Q^2, permutation tests, VIP > 1), and model-validation metrics (accuracy, balanced accuracy, precision, recall, and F1-score). This framework is designed to identify recurrent high-importance markers for Xinjiang terroir recognition – particularly coupled hydroclimatic-geochemical signals such as δ^{18}O, Li,

Na, and Sr – and to support GI-oriented authenticity control in an arid oasis-desert viticultural system.

MATERIALS AND METHODS

1. Sample collection and preparation

A total of 473 wine samples (Table 1 shows) were collected from seven sub-regions of Xinjiang, China, namely Changji (30), Hami (50), Heshuo (106), Kuerle (20), Shihezi (46), Wujiaqu (130), and Yanqi (91); Figure 1 provides a geographical overview of the regions from which Xinjiang wine samples were collected. All samples were obtained during the 2022 vintage, representing both commercial wines released in the local market and experimental wines produced under standardised vinification procedures. Samples were collected directly from sealed bottles provided by wineries or official distributors to guarantee authenticity. Each bottle was coded with a random three-digit number to anonymise regional identity during subsequent analyses. Prior to analysis, bottles were stored in a dark cellar at 12 ± 2 °C and 65–70 % relative humidity to maintain quality.

TABLE 1. Summary of Xinjiang wine samples by region: sample size (n), all grape cultivars with sample counts, and vintage range.

Region	Sample size	Cultivars	Vintage range
Changji	30	Cabernet-Sauvignon (15); Chardonnay (10); Pinot noir (5)	2022
Hami	50	Chardonnay (10); Italian Riesling (10); Cabernet-Sauvignon (10); Syrah (10); Merlot (10)	2022
Heshuo	106	Cabernet-Sauvignon (40); Riesling (20); Merlot (16); Chardonnay (10); Cabernet-Sauvignon/Merlot (10); Syrah (5); Italian Riesling (5)	2022
Kuerle	20	Cabernet-Sauvignon (10); Cabernet franc (10)	2022
Shihezi	46	Chardonnay (10); Riesling (10); Italian Riesling (10); Merlot (8); Cabernet-Sauvignon (8)	2022
Wujiaqu	130	Cabernet-Sauvignon (30); Merlot (20); Italian Riesling (15); Riesling (15); Chardonnay (15); Cabernet-Sauvignon/Merlot (15); Riesling/Chardonnay (5); Petit Manseng (5); Petit Verdot (5); Syrah (5)	2022
Yanqi	91	Cabernet-Sauvignon (35); Merlot (16); Syrah (15); Italian Riesling/Riesling (10); Cabernet-Sauvignon/Merlot (10); Cabernet Gernischt (5)	2022

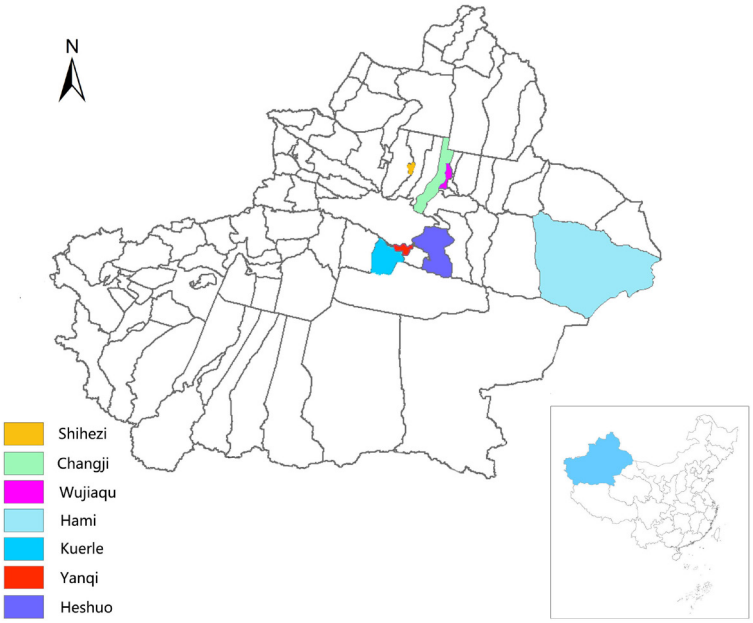


FIGURE 1. Geographic distribution of wine sampling across seven Xinjiang regions – Shihezi, Changji, Wujiaqu, Hami, Kuerle, Yanqi, and Heshuo.

2. Multielement analysis

2.1. Sample pretreatment

Wine samples were pretreated following established protocols. Carbon dioxide in sparkling wines was removed by ultrasonic treatment (Zheng *et al.*, 2025). Aliquots (5.0 mL) of each sample (red, *rosé*, sparkling, and white) were placed into Teflon digestion vessels, concentrated to 1.0 mL, and mixed with 3 mL concentrated HNO_3. The sealed vessels were digested for ≥ 4 h until the solutions became nearly colourless. After cooling, digests were transferred to 50 mL volumetric flasks, rinsed with Milli-Q water, and diluted to volume. Prior to potassium determination, solutions were further diluted 100-fold. All vessels and flasks were pre-cleaned with 5 % HNO_3 to avoid cross-contamination.

2.2. Determination of elemental concentrations

Twenty-seven elements (Na, Mg, K, Ca, Li, Al, V, Cr, Mn, Fe, Co, Ni, Cu, Zn, As, Mo, Sn, Sb, Ba, Rb, Sr, Y, Cs, Ce, Pb, Th, and U) were quantified in wine samples using ICP-MS (PerkinElmer Nexion 300X, USA) (Almeida & Vasconcelos, 2003). Operating conditions followed previous studies. Calibration was performed with mixed standard solutions (Cu, Mn, Zn, Ba; V, Cr, Co, Ni, As, Pb; and Ca, Mg, Na, 100 µg/mL each) and single-element standards (1000 µg/mL) for the remaining elements. All analyses were conducted in triplicate.

2.3. Measurement of stable isotope ratios

The stable isotope ratios of oxygen ($\delta^{18}O$) in water and carbon ($\delta^{13}C$) in ethanol from wine samples were expressed relative to the international standard Vienna Pee Dee Belemnite (VPDB) and calculated as:

$$\delta^{18}O\text{sample (‰)} \text{ or } \delta^{13}C\text{sample (‰)} = [(Rs/Rst) - 1] \times 1000$$

where Rs denotes the isotope ratio ($^{18}O/^{16}O$ or $^{13}C/^{12}C$) of the sample, and Rst represents that of the standard. Results are reported as δ (‰) values relative to VPDB. The determination of $\delta^{18}O$ and $\delta^{13}C$ followed the referenced method (Leder *et al.,* 2021). Wine samples were directly injected into an EA/LC-IRMS system (Delta V Advantage, Thermo Fisher Scientific, USA). All measurements were performed in triplicate. For quality control, a reference material was analysed at the beginning and end of each sequence, as well as after every eight samples.

2.4. Data analysis

All elemental and isotopic data ($\delta^{13}C$, $\delta^{18}O$) were merged and standardised (*z*-scores) before analysis. PCA was first applied to visualise clustering trends, followed by OPLS-DA to enhance regional discrimination and identify key variables (VIP > 1). Four supervised algorithms – Random Forest (RF), Artificial Neural Network (ANN), Support Vector Machine (SVM), and Recursive Partitioning Tree (R-Part) – were used for classification, with 10-fold cross-validation to evaluate accuracy and robustness. Data analysis and visualisation were performed using R (mixOmics, randomForest, ggplot2) and Python (Matplotlib) (Guo *et al*., 2021).

RESULTS

1. Multi-element and stable isotope signatures of wines from seven Xinjiang sub-regions

Significant spatial variations were observed in elemental compositions among the studied Xinjiang wine sub-regions (Table 2). Among alkali metals, Li concentrations differed markedly, with Wujiaqu exhibiting the highest mean value (112.81 ± 32.10 µg/L), nearly twice that measured in Shihezi (48.73 ± 7.07 µg/L). Sodium concentrations were also relatively elevated in Wujiaqu, whereas K reached its maximum level in Kuerle (2034.48 ± 124.63 µg/L), exceeding those recorded in other regions. Alkaline earth metals showed moderate interregional variability. Mg concentrations were highest in Hami (169.38 ± 28.96 µg/L), while Ca concentrations exhibited less pronounced differences, with relatively higher mean values in Changji, Wujiaqu, and Hami. Transition metals displayed substantial spatial heterogeneity. Al concentrations were notably higher in Changji (1047.46 ± 440.70 µg/L) and Wujiaqu (983.61 ± 590.26 µg/L), whereas Kuerle showed comparatively lower levels. Vanadium concentrations reached their highest mean values in Heshuo, while Cr was most enriched in Changji. Copper concentrations varied considerably among regions, with the highest mean Cu level observed in Hami (419.55 ± 147.96 µg/L). Trace elements further contributed to regional differentiation. Sr concentrations were relatively higher in Hami and Wujiaqu, whereas Rb exhibited a pronounced enrichment in Yanqi, contrasting with lower levels in Hami and Wujiaqu. Stable isotope ratios also exhibited clear spatial patterns. $\delta^{13}C$ values were most enriched in Kuerle wines (–26.46 ± 0.60 ‰), while more negative values were observed in Changji and Wujiaqu (approximately –28 ‰). $\delta^{18}O$ values were highest in Heshuo, followed by Kuerle and Wujiaqu, with lower values recorded in Shihezi and Yanqi.

2. Environmental drivers of isotopic enrichment and elemental differentiation in Xinjiang wines

To investigate environmental controls on isotopic enrichment and elemental differentiation among Xinjiang wines, correlation analyses were conducted between geochemical variables (27 elements and two stable isotopes) and key climatic parameters (Table S1 shows), including mean annual precipitation, evaporation, temperature, and sunshine duration (Table 3). Both Pearson (r) and Spearman (ρ) correlation coefficients were calculated to evaluate the consistency of linear and monotonic relationships.

Among isotopic indicators, $\delta^{18}O$ showed a strong positive correlation with annual evaporation (r = 0.626; ρ = 0.714), whereas $\delta^{13}C$ exhibited a moderate positive correlation with mean temperature (r = 0.472; ρ = 0.429). Several elemental variables also displayed clear climatic sensitivities. Al was strongly negatively correlated with temperature (r = –0.757; ρ = –0.714). Na and Mg were positively associated with sunshine duration, with Na showing r = 0.359 and ρ = 0.607, and Mg showing r = 0.653 and ρ = 0.500. Overall, Pearson and Spearman coefficients exhibited highly consistent trends across variables.

TABLE 2. Concentrations of 27 elements (mg·kg^{-1}) and two stable isotopes (‰) in wine samples from seven Xinjiang sub-regions (mean ± SD). (part 1/2)

Reginal marker	Shehezi (n = 46)	Wujiaqu (n = 130)	Changji (n = 30)	Hami (n = 50)	Kuerle (n = 20)	Heshuo (n = 106)	Yanqi (n = 91)
Li	48.73 ± 7.07^{a}	112.81 ± 32.10^{b}	81.89 ± 69.61^{bc}	62.16 ± 26.35^{bc}	73.17 ± 36.29^{bc}	58.24 ± 26.20	60.36 ± 24.76^{bc}
Na	20.91 ± 8.33^{a}	54.64 ± 24.57^{b}	28.40 ± 7.07^{c}	40.46 ± 18.45^{cd}	28.41 ± 9.74^{c}	39.70 ± 13.02^{cd}	33.32 ± 14.49^{cd}
Mg	119.90 ± 28.01^{a}	151.22 ± 32.59^{ab}	141.16 ± 36.51^{ab}	169.38 ± 28.96^{c}	105.41 ± 43.60^{a}	138.21 ± 19.23^{ab}	143.23 ± 20.49^{ab}
Al	504.24 ± 313.33^{a}	983.61 ± 590.26^{b}	1047.46 ± 440.70^{b}	688.26 ± 425.49^{bc}	279.18 ± 109.59^{d}	755.21 ± 607.66^{bc}	694.81 ± 391.23^{bc}
K	1514.77 ± 360.44^{a}	1887.93 ± 588.33^{ab}	1736.38 ± 707.29^{ab}	1511.03 ± 511.42^{a}	2034.48 ± 124.63^{b}	1265.47 ± 467.17^{bc}	1586.85 ± 343.55^{a}
Ca	68.32 ± 6.80^{a}	84.62 ± 17.82^{ab}	93.28 ± 80.81^{bc}	88.63 ± 19.52^{bc}	63.09 ± 30.85^{a}	72.99 ± 20.97^{ab}	79.07 ± 11.98^{ab}
V	4.96 ± 7.76^{ab}	3.10 ± 3.81^{a}	10.17 ± 13.53^{bc}	14.88 ± 12.53^{c}	7.71 ± 4.67^{ab}	30.37 ± 26.89^{d}	12.16 ± 15.39^{bc}
Cr	14.84 ± 4.04^{ab}	16.02 ± 8.93^{bc}	46.31 ± 61.06^{d}	19.84 ± 8.48^{c}	8.24 ± 3.78^{a}	21.70 ± 8.72^{c}	17.65 ± 7.98^{a}
Mn	1274.62 ± 360.89^{bc}	1306.15 ± 342.50^{bc}	1434.79 ± 603.40^{cd}	1391.15 ± 356.97^{bc}	627.70 ± 245.23^{a}	1064.32 ± 370.68^{b}	1630.32 ± 538.21^{d}
Fe	1369.05 ± 1118.32^{a}	2532.57 ± 1919.90^{c}	1706.93 ± 1090.91^{ab}	2658.28 ± 1789.12	2381.41 ± 668.61^{bc}	1828.31 ± 859.84^{b}	2698.29 ± 909.01^{c}
Co	3.26 ± 0.78^{ab}	3.51 ± 1.30^{b}	4.06 ± 1.29^{c}	4.44 ± 1.72	1.29 ± 0.54^{a}	3.15 ± 1.12^{ab}	3.72 ± 1.55^{bc}
Ni	15.91 ± 5.53^{b}	20.47 ± 6.66^{bc}	29.59 ± 15.81^{c}	18.60 ± 6.21^{ab}	9.14 ± 4.05^{a}	19.25 ± 10.95^{ab}	15.58 ± 5.07^{b}
Cu	124.77 ± 30.35^{b}	264.51 ± 203.91^{c}	49.63 ± 39.9^{4a}	419.55 ± 147.96^{e}	304.76 ± 101.02^{d}	162.68 ± 113.86^{bc}	162.58 ± 178.41^{bc}
Zn	457.23 ± 84.57^{bc}	488.00 ± 170.82^{c}	509.03 ± 175.96^{cd}	371.33 ± 190.94^{b}	134.39 ± 83.35^{a}	325.89 ± 157.53^{b}	464.49 ± 256.75^{bc}

TABLE 2. Concentrations of 27 elements (mg·kg^{-1}) and two stable isotopes (‰) in wine samples from seven Xinjiang sub-regions (mean ± SD). (part 2/2)

As	3.56 ± 2.72^{b}	4.18 ± 1.50^{bc}	3.67 ± 2.49^{b}	4.99 ± 0.95^{bc}	1.82 ± 1.36^{a}	6.38 ± 2.74^{c}	3.45 ± 1.87^{b}
Mo	1.87 ± 3.33^{b}	8.02 ± 12.48^{c}	1.79 ± 3.64^{b}	8.69 ± 7.35^{c}	0.18 ± 0.30^{a}	1.43 ± 3.44^{b}	0.55 ± 1.98^{ab}
Sn	1.31 ± 1.41^{a}	4.15 ± 5.27^{ab}	16.99 ± 21.58^{c}	2.63 ± 2.08^{a}	5.70 ± 2.29	4.15 ± 3.91^{ab}	7.63 ± 7.98^{b}
Sb	0.29 ± 0.22^{cd}	0.35 ± 0.20^{d}	0.25 ± 0.19^{c}	0.23 ± 0.20^{c}	0.01 ± 0.01^{a}	0.09 ± 0.16^{b}	0.15 ± 0.22^{bc}
Ba	77.41 ± 28.78^{bc}	97.64 ± 32.89^{c}	94.81 ± 25.94^{c}	67.63 ± 17.75^{b}	42.25 ± 17.33^{a}	70.67 ± 31.56^{bc}	105.72 ± 59.84^{cd}
Rb	1375.19 ± 444.72^{b}	1070.93 ± 376.35^{a}	1489.45 ± 566.85^{bc}	1049.31 ± 581.97^{a}	1199.21 ± 536.27^{ab}	1269.99 ± 480.71^{ab}	1633.77 ± 829.63^{c}
Sr	104.54 ± 33.67^{a}	208.16 ± 59.32^{c}	159.64 ± 137.05^{bc}	223.24 ± 44.21^{cd}	164.73 ± 51.95^{bc}	134.23 ± 47.17^{ab}	143.75 ± 48.39^{b}
Y	0.32 ± 0.25^{ab}	0.71 ± 0.45^{c}	0.73 ± 0.45^{c}	0.47 ± 0.21^{bc}	0.23 ± 0.15^{a}	0.91 ± 0.92^{cd}	0.50 ± 0.35^{bc}
Cs	5.01 ± 1.24^{bc}	1.91 ± 1.22^{a}	3.74 ± 1.50^{ab}	3.12 ± 2.69^{ab}	4.88 ± 1.85^{bc}	4.22 ± 1.88^{bc}	15.55 ± 15.07^{d}
Ce	0.33 ± 0.33^{a}	0.46 ± 0.45^{ab}	0.48 ± 0.56^{ab}	0.60 ± 0.34^{bc}	0.51 ± 0.39^{b}	1.20 ± 0.91^{c}	0.49 ± 0.45^{ab}
Pb	6.37 ± 3.73^{ab}	7.60 ± 3.84^{b}	7.57 ± 5.49^{b}	4.20 ± 2.48^{a}	3.93 ± 1.76^{a}	5.62 ± 3.43^{ab}	9.05 ± 6.76^{bc}
Th	0.04 ± 0.04^{a}	0.07 ± 0.07^{ab}	0.05 ± 0.05^{ab}	0.02 ± 0.03^{a}	0.09 ± 0.09^{b}	0.16 ± 0.15^{c}	0.08 ± 0.08^{b}
U	0.17 ± 0.14^{a}	0.19 ± 0.21^{a}	0.33 ± 0.40^{ab}	0.20 ± 0.11^{a}	0.40 ± 0.22	0.69 ± 0.82^{b}	0.21 ± 0.19^{a}
δ^{13}C	–27.15 ± 0.55^{a}	–28.00 ± 0.72^{ab}	–28.09 ± 0.53^{ab}	–27.59 ± 0.60^{a}	–26.46 ± 0.60^{a}	–28.82 ± 1.18^{ab}	–27.10 ± 1.39^{a}
δ^{18}O	4.55 ± 1.71^{a}	6.15 ± 1.59^{ab}	4.76 ± 2.56^{a}	5.67 ± 1.72^{ab}	6.63 ± 0.37^{b}	7.48 ± 2.40^{bc}	4.49 ± 2.91^{a}

TABLE 3. Pearson and Spearman correlation coefficients between isotopic/elemental variables and climatic parameters.

Variable	Precipitation (r/ρ)	Evaporation (r/ρ)	Temperature (r/ρ)	Sunshine (r/ρ)
Li	0.35/–0.14	0.18/0.32	–0.39/–0.32	–0.20/–0.07
Na	–0.07/–0.39	0.32/0.29	–0.17/0.00	0.36/0.61
Mg	0.00/–0.07	0.12/–0.07	–0.23/–0.29	0.65/0.50
Al	0.52/0.46	–0.20/–0.21	–0.76/–0.71	–0.04/–0.14
K	0.11/–0.14	0.28/0.11	0.09/–0.18	–0.30/–0.36
Ca	0.32/0.21	0.03/–0.04	–0.46/–0.46	0.31/0.14
$\delta^{13}C$	–0.24/–0.46	0.06/0.00	0.47/0.43	–0.08/0.11
$\delta^{18}O$	–0.46/–0.36	0.63/0.71	0.43/0.36	0.23/0.14

Note: Bold values indicate strong correlations (|r| or |ρ| ≥ 0.6).

3. PCA and OPLS-DA analysis

To evaluate the discriminative potential of multi-elemental and stable isotopic variables for differentiating the seven Xinjiang wine-producing sub-regions, principal component analysis (PCA) was first conducted on standardised data. The PCA score plot (Figure 2) indicated that the first two principal components explained 36.9 % of the total variance (PC1 = 19.8 %, PC2 = 17.1 %). Samples from different sub-regions were distributed across the PC1-PC2 space, showing partial separation. Wines from Hami (HMI) and Kuerle (KRL) formed distinct clusters along PC1, whereas Shihezi (SHZ) and Wujiaqu (WJQ) partially overlapped, suggesting similarities in their isotope-element fingerprints.

To improve regional discrimination, orthogonal partial least squares-discriminant analysis (OPLS-DA) was subsequently applied. The OPLS-DA model included one predictive and one orthogonal component, with $R^2X = 0.143$, $R^2Y = 0.166$, and $Q^2 = 0.151$, indicating a modest but meaningful supervised discrimination signal. Here, R^2X and R^2Y represent the explained variance of the predictor matrix (isotope-element variables) and response matrix (sub-regional classes), respectively, whereas Q2 reflects cross-validated predictive ability. Given the complexity of natural wine matrices and partial overlap among some sub-regions, these values were interpreted together with permutation testing, VIP-based marker selection, PCA patterns, and machine-learning

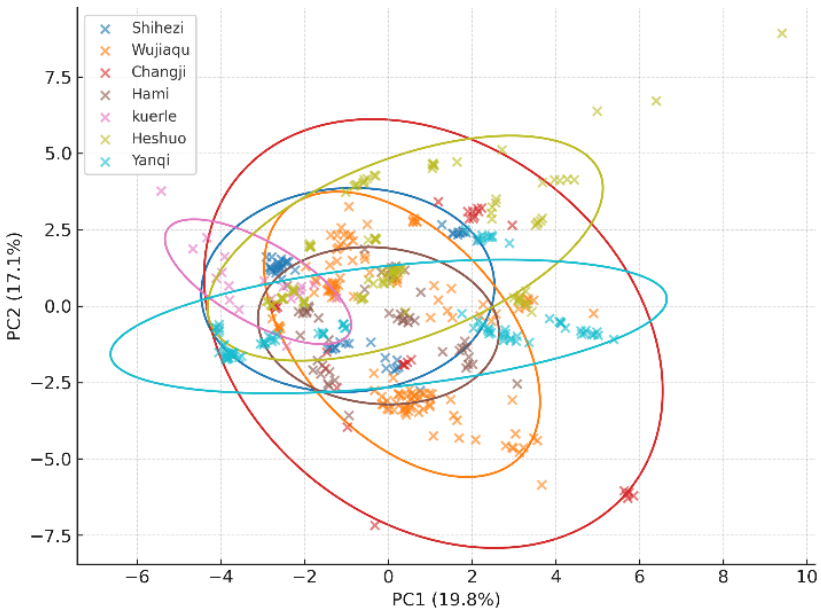


FIGURE 2. Principal component analysis (PCA) score plot of Xinjiang wines based on elemental and isotopic compositions.

classification results. The OPLS-DA score plot (Figure 3A) showed improved separation along the predictive component relative to PCA. HMI and Yanqi (YQ) samples tended to cluster compactly, whereas SHZ, WJQ, and Changji (CJ) exhibited partial overlap.

Variable importance in projection (VIP) analysis (Figure 3B) identified the main discriminant variables (VIP > 1), including alkali and alkaline earth elements (Li, Na, K, Sr), selected transition/trace elements (*e.g.*, Cu, V, Mn, As), and the stable isotope $\delta^{18}O$. Among these, Li, Na, K, and Sr consistently ranked among the highest VIP scores. $\delta^{18}O$ also displayed a high VIP value.

4. Integration of multi-elemental and isotopic fingerprints for regional discrimination

To further evaluate the discriminative capacity of integrated multi-elemental and isotopic fingerprints across the seven Xinjiang wine sub-regions, four supervised classification algorithms – Random Forest (RF), Artificial Neural Network (ANN), Support Vector Machine (SVM), and Recursive Partitioning (R-Part) – were applied. These approaches are widely used for geographical origin traceability in wine and other agricultural products, often providing robust classification performance (Hassan *et al.*, 2025; Li J. *et al.*, 2025; Ranaweera *et al.*, 2021a; Sun *et al.*, 2022). All models were trained using standardised elemental

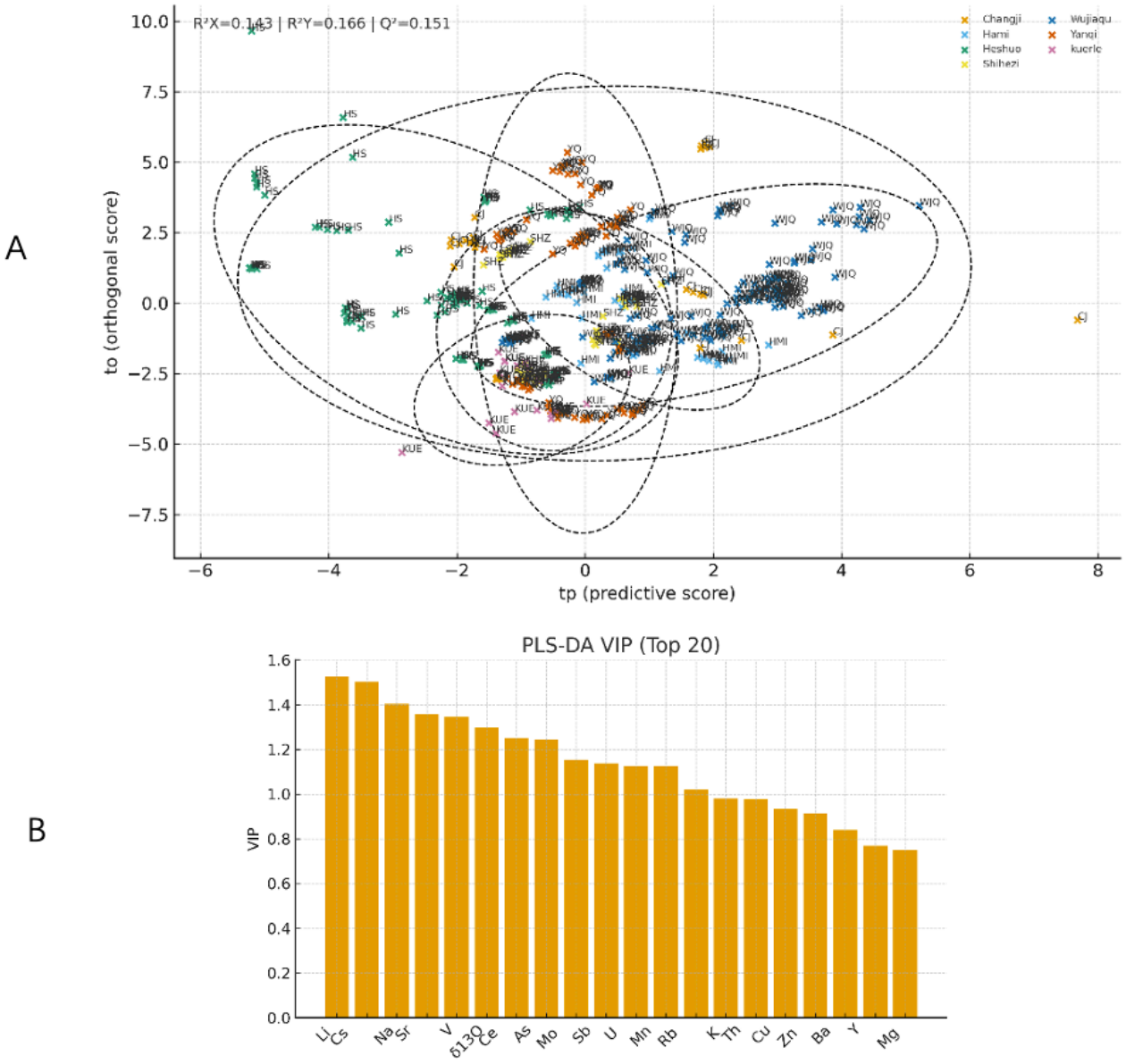


FIGURE 3. (A) OPLS-DA score plot showing the discrimination of wine samples from seven Xinjiang sub-regions based on elemental and isotopic compositions; (B) Variable importance in projection (VIP) scores of the top 20 variables contributing to the OPLS-DA model.

and isotopic variables, and predictive performance was assessed by cross-validation (Table 4). Among the tested algorithms, RF achieved the highest overall classification accuracy (92 %), followed by ANN (88 %), SVM (86 %), and R-Part (79 %).

Across all models, a consistent set of predictors emerged as major contributors to regional discrimination (Table 4). Alkali and alkaline earth elements – particularly Li, Na, and Sr – were repeatedly ranked among the top variables, together with selected transition and trace elements (*e.g.*, V, Cu, Mn, As), and the stable isotope $\delta^{18}O$. Notably, $\delta^{18}O$ was frequently selected among the top contributors across RF, ANN, SVM, and R-Part models.

DISCUSSION

1. Geochemical and climatic drivers of element-isotope variability across Xinjiang sub-regions

The observed spatial variability in elemental composition highlights the geochemical heterogeneity among Xinjiang wine-producing sub-regions. The pronounced enrichment of Li in Wujiaqu, together with elevated Na levels, may reflect differences in geological background or irrigation water composition, which have been reported to influence alkali metal signatures in wines from arid regions (Hu *et al*., 2019; Li Y. *et al*., 2023). In contrast, the high K concentrations observed in Kuerle are consistent with its distinct elemental profile and may be associated with enhanced ion accumulation under dry climatic conditions (Li Y. *et al*., 2023). Moderate regional variability in Mg and Ca likely reflects differences in geological substrate, soil mineral composition, and irrigation-water sources. In our dataset, the relatively overlapping Ca ranges indicate a more conservative (less discriminant) behaviour of Ca compared with more variable alkali-related markers. This interpretation is consistent with previous multi-element wine traceability studies showing that elemental profiles capture regional geochemical signals relevant to origin discrimination (Rapa *et al*., 2023). The strong heterogeneity observed for transition metals, particularly Al, V, Cr, and Cu, further emphasises the complexity of regional geochemical inputs. Elevated Al levels in Changji and Wujiaqu are consistent with areas influenced by loess-derived materials, while the higher Cu concentrations detected in Hami may partially reflect cumulative inputs from viticultural or winemaking practices, in addition to natural background levels. Trace elements such as Sr and Rb provided additional discriminatory power, as their contrasting enrichment patterns among regions suggest sensitivity to local soil and parent material characteristics (Rapa *et al*., 2023). These elements have been widely reported as robust geographical tracers in wine provenance studies (Durante *et al*., 2016; Gonzálvez *et al.*, 2009; Pilgrim *et al.*, 2010). Stable isotope results revealed coherent climatic gradients across the study area (Gouveia *et al.*, 2019; Santesteban *et al*., 2015). The relatively enriched $\delta^{13}C$ values observed in Kuerle wines are consistent with increased vine water stress and higher water-use efficiency, whereas more negative $\delta^{13}C$ values in Changji and Wujiaqu suggest comparatively less severe water limitation (Gao *et al*., 2025). Similarly, the enrichment of $\delta^{18}O$ in Heshuo and Kuerle aligns with enhanced evaporative effects under arid conditions. Collectively, $\delta^{13}C$ and $\delta^{18}O$ act as sensitive indicators of regional water status, complementing elemental fingerprints for differentiating Xinjiang wine sub-regions.

2. Climate-geochemistry interactions underpinning regional chemical fingerprints

The strong positive association between $\delta^{18}O$ and evaporation supports the interpretation that oxygen isotope enrichment is closely linked to evaporative processes under arid climates, consistent with previous reports (Pang *et al*., 2011). In contrast, the moderate positive correlation between $\delta^{13}C$ and temperature suggests that warmer environments are associated with less negative $\delta^{13}C$ values, likely reflecting regional differences in vine water status; similar patterns have been reported elsewhere (Kingston *et al*., 2025; Pereira *et al*., 2025).

Elemental responses further indicate that climate-related processes contribute to the observed chemical differentiation. The strong negative relationship between Al and temperature may imply reduced aluminosilicate-related inputs or altered particle availability under warmer conditions. Meanwhile, the positive correlations of Na and Mg with sunshine duration suggest that enhanced solar radiation and associated evapotranspiration may promote the concentration of soluble elements in surface soils and water sources (Feng & Xiang-Ling, 2025). The close agreement between Pearson and Spearman coefficients indicates that these climate-geochemistry relationships are largely linear or monotonic.

Collectively, these results highlight the prominent role of climatic aridity – particularly evaporation, temperature and solar radiation – in shaping isotopic enrichment and elemental differentiation among Xinjiang wine-producing sub-regions (Abdennour *et al*., 2021; Feng & Xiang-Ling, 2025).

TABLE 4. Performance comparison of four classification models for regional discrimination of Xinjiang wines.

Model	Cross-validation accuracy	Top contributing variables
RF	92 %	Li, Na, Sr, V, Cs, Cu, K, Mn, As, $\delta^{18}O$
ANN	88 %	$\delta^{18}O$, Li, Cs, Sr, V, Na
SVM	86 %	Li, Sr, $\delta^{18}O$, Cs, V, Cu
R-Part	79 %	Sr, $\delta^{18}O$, Na, Cs

Importantly, the climatic sensitivities revealed by correlation analysis align with multivariate classification outcomes (Table 4): variables strongly associated with climatic gradients (*e.g.*, Li, Na, Sr, selected transition metals, and $\delta^{18}O$) consistently ranked among the top contributors in Random Forest, Artificial Neural Network, Support Vector Machine, and Recursive Partitioning Models. This convergence between univariate climatic correlations and multivariate discrimination performance reinforces the central role of climate-geochemistry interactions in defining regional chemical fingerprints and provides a robust basis for provenance discrimination and terroir characterisation of Xinjiang wines.

3. Interpreting PCA and OPLS-DA: key drivers of sub-regional discrimination

The partial clustering observed in PCA indicates that integrated elemental-isotopic features capture regional geochemical differentiation to some extent, although unsupervised separation remained incomplete. The overlap between SHZ and WJQ may reflect shared climatic and soil characteristics, particularly within oasis-irrigated areas influenced by similar parent material composition (Abdennour *et al*., 2021). These findings support the need for supervised approaches to enhance discrimination accuracy (Rapa *et al.*, 2024).

OPLS-DA improved sub-regional separation and highlighted a limited set of variables driving discrimination. The prominence of alkali and alkaline earth elements (Li, Na, K, Sr) suggests that regional geochemical background and water-soil interactions contribute strongly to the observed differentiation. In particular, Na and K – often sensitive to evaporative concentration under arid conditions – supported separation of samples from more arid basins, whereas Sr, frequently associated with carbonate substrates and groundwater inputs, provided additional discriminatory power across alluvial settings. The appearance of transition and trace elements (*e.g.*, Cu, V, Mn, As) among top-ranked variables indicates that multi-element fingerprints reflect combined effects of natural geochemical variability together with integrated vineyard-winemaking inputs, rather than single-source controls. The high VIP value of $\delta^{18}O$ is consistent with its sensitivity to regional climatic conditions, especially evaporation intensity. Together, the concurrent importance of $\delta^{18}O$ and climate-responsive elemental variables supports the interpretation that climate-modulated hydrological and geochemical processes jointly shape regional wine fingerprints.

Overall, these multivariate patterns reinforce that both geogenic and climatic factors underpin the elemental-isotopic composition of Xinjiang wines, highlighting a strong environmental imprint of regional terroir (Feng & Xiang-Ling, 2025). However, the residual overlap among neighbouring oasis regions suggests that viticultural practices and irrigation management may partially obscure purely geochemical differentiation (Cataldo *et al.*, 2021; Santagostini & Guglielmi, 2024). In a broader interpretation, arid regions such as HMI and KRL tended to be characterised by higher Na, K, $\delta^{13}C$, and $\delta^{18}O$ values; oasis-irrigated areas (SHZ, WJQ) by relatively elevated Sr, Ca, and Rb; and central regions (CJ, YQ) by more balanced compositions with lower isotope ratios. Collectively, the PCA and OPLS-DA results provide a robust geochemical basis for regional classification and origin authentication of Xinjiang wines, and offer quantitative evidence to support terroir characterisation and differentiated quality management within this rapidly developing wine region.

4. Machine-learning integration of element-isotope fingerprints for regional discrimination

The superior performance of RF suggests that ensemble-based learning is particularly effective for capturing complex, potentially non-linear relationships in high-dimensional elemental-isotopic datasets. ANN and SVM also achieved high accuracies, supporting the robustness of supervised learning for sub-regional discrimination, whereas R-Part provided a more transparent decision structure but at the cost of reduced predictive performance. Despite differences in model architecture and decision logic, the convergence in top contributing variables indicates stability and interpretability of the integrated modelling framework (Ranaweera *et al.*, 2021b).

The recurrent importance of Li, Na, and Sr highlights the dominant influence of regional geochemical background and water-related processes on chemical differentiation among Xinjiang sub-regions (Abdennour *et al*., 2021). In parallel, the frequent selection of $\delta^{18}O$ across all classifiers indicates that climate-sensitive isotopic signals – particularly those shaped by evaporative conditions – provide strong discriminatory power. When interpreted together with PCA and OPLS-DA, the machine-learning results confirm a coherent multi-level discrimination pattern: PCA captured the overall structure of regional variability, OPLS-DA enhanced separation and identified key discriminant variables, and RF delivered the highest predictive accuracy, demonstrating complementary strengths among unsupervised, supervised, and ensemble-based approaches.

Overall, integrating elemental and isotopic information with multiple supervised algorithms provides a robust and reproducible framework for regional discrimination of Xinjiang wines. The consistent identification of a limited set of climate- and geochemistry-sensitive variables further supports the suitability of multi-elemental and isotopic fingerprints for terroir-oriented wine traceability in arid continental viticultural regions (Feng & Xiang-Ling, 2025).

Nevertheless, several limitations should be acknowledged. The present dataset covers seven major Xinjiang sub-regions but excludes the Ili Valley; therefore, the conclusions are most directly applicable to the sampled macro-zones (Northern Tianshan, Yanqi Basin, and Tuha Basin). Intra-regional heterogeneity (vineyard management, irrigation regime, and cultivar composition) was not fully resolved and may contribute to residual overlap among some groups (Bai *et al*., 2025; Feng & Xiang-Ling, 2025). In addition, all samples were from a single vintage (2022), and marker

stability across years remains untested. Elemental profiles in bottled wines reflect integrated vineyard and winery inputs, with minor packaging effects. Although analytical contamination was minimised (acid-cleaned vessels, controlled Teflon digestion, triplicate QC), source attribution to single environmental drivers should be interpreted cautiously (Hu *et al*., 2019). The ICP-MS panel also excluded S and P, and no paired soil or irrigation-water samples were available, limiting mechanistic apportionment. Comparisons with published datasets and OIV limits are included as context only, as this study targets origin authentication rather than compliance testing. Future work should use multi-vintage, paired soil-water-grape-wine designs and radiogenic isotope systems ($^{87}Sr/^{86}Sr$; Sr-Pb) to improve transferability and terroir-oriented geotraceability (Epova *et al*., 2019; Cellier *et al*., 2021; Erban Kochergina *et al*., 2024).

ACKNOWLEDGEMENTS

This work was supported by SZPU Research Project-6024330001K and the Key Wine Research Project (AKYZD1906-3).

DECLARATION OF CONFLICTING INTERESTS

The authors declare that they have no known financial conflicts of interest or personal relationships that could have influenced the work presented in this article.

REFERENCES

Abdennour, M. A., Douaoui, A., Barrena, J., Pulido, M., Bradaï, A., Bennacer, A., Piccini, C., & Alfonso-Torreño, A. (2021). Geochemical characterization of the salinity of irrigated soils in arid regions (Biskra, SE Algeria). Acta Geochimica, 40(2), 234–250. https://doi.org/10.1007/s11631-020-00426-2

Almeida, C. M. R., & Vasconcelos, M. T. S. (2003). Multielement composition of wines and their precursors including provenance soil and their potentialities as fingerprints of wine origin. Journal of Agricultural and Food Chemistry, 51(16), 4788–4798. https://doi.org/10.1021/jf034145b

Anderson, K. (2025). China's wine markets: What next? Australian and New Zealand Grapegrower and Winemaker, 733, 80–85.

Bai, L., Zhang, Z., Li, Y., Zhao, S., Yang, X., Chen, C., Zhao, S., Zhang, P., Peng, X., & Zhao, Y. (2025). Combining stable isotopes and multi-elements with machine learning chemometric models to identify the geographical origins of Tetrastigma hemsleyanum Diels et Gilg. Food Chemistry, 469, 142496. https://doi.org/10.1016/j.foodchem.2024.142496

Cataldo, E., Fucile, M., & Mattii, G. B. (2021). A review: Soil management, sustainable strategies and approaches to improve the quality of modern viticulture. Agronomy, 11(11), 2359. https://doi.org/10.3390/agronomy11112359

Cellier, R., Berail, S., Barre, J., Epova, E., Claverie, F., Ronzani, A.-L., Milcent, S., Ors, P., & Donard, O. F. X. (2021). Analytical strategies for Sr and Pb isotopic signatures by MC-ICP-MS applied to the authentication of Champagne and other sparkling wines. Talanta, 234, 122433. https://doi.org/10.1016/j.talanta.2021.122433

Coetzee, P., Van Jaarsveld, F., & Vanhaecke, F. (2014). Intraregional classification of wine via ICP-MS elemental fingerprinting. Food Chemistry, 164, 485–492. https://doi.org/10.1016/j.foodchem.2014.05.027

Crespo-Moncada, B., Posada-Izquierdo, G. D., Velásquez-Rivera, J., Molina-Villamar, J., & García-Gimeno, R. M. (2025). Geographical Indication Labels for Food Products: A Literature Review. Encyclopedia, 5(3), 115. https://doi.org/10.3390/encyclopedia5030115

Day, M., & Wilkes, E. (2021). Development of tools to verify origin and varietal nature of wines (Final report to Wine Australia, Project No. AWRI 1701-4.4.2). The Australian Wine Research Institute (AWRI) and Wine Australia. https://www.wineaustralia.com/getmedia/b7b85a59-af85-4d38-a0fa-86886cd32679/AWR-1701-4-4-2-Final-Report.pdf

Durante, C., Bertacchini, L., Bontempo, L., Camin, F., Manzini, D., Lambertini, P., Marchetti, A., & Paolini, M. (2016). From soil to grape and wine: Variation of light and heavy elements isotope ratios. Food Chemistry, 210, 648–659. https://doi.org/10.1016/j.foodchem.2016.04.108

Epova, E. N., Bérail, S., Séby, F., Vacchina, V., Bareille, G., Médina, B., Sarthou, L., & Donard, O. F. X. (2019). Strontium elemental and isotopic signatures of Bordeaux wines for authenticity and geographical origin assessment. Food Chemistry, 294, 35–45. https://doi.org/10.1016/j.foodchem.2019.04.068

Erban Kochergina, Y. V., Pavloušek, P., Šanda, M., & Hora, J. M. (2024). 87Sr/86Sr isotopic composition of wine: Uses and limitations. OENO One, 58(2), 1–15. https://doi.org/10.20870/oeno-one.2024.58.2.7451

Feng, X., & Xiang-Ling, T. (2025). Climatic zoning of Xinjiang for heterogeneous production of high-quality wine. Scientific Reports, 15(1), 2929. https://doi.org/10.1038/s41598-025-86907-x

Gao, F., Zeng, G., Hao, X., Wang, H., & Li, H. (2025). Variation and fractionation of δ2H, δ18O, and δ17O stable isotopes from irrigation water to soil, grapes, and wine for the traceability of geographical origins. Food Chemistry, 462, 141012. https://doi.org/10.1016/j.foodchem.2024.141012

Gonzálvez, A., Llorens, A., Cervera, M. L., Armenta, S., & de la Guardia, M. (2009). Elemental fingerprint of wines from the protected designation of origin Valencia. Food Chemistry, 112(1), 26–34. https://doi.org/10.1016/j.foodchem.2008.05.043

Gouveia, C. S., Ganança, J. F., Slaski, J., Lebot, V., & de Carvalho, M. Â. P. (2019). Stable isotope natural abundances (δ13C and δ15N) and carbon-water relations as drought stress mechanism response of taro (Colocasia esculenta L. Schott). Journal of Plant Physiology, 232, 100–106. https://doi.org/10.1016/j.jplph.2018.11.024

Guan, J., Yao, J., Li, M., Li, D., & Zheng, J. (2022). Historical changes and projected trends of extreme climate events in Xinjiang, China. Climate Dynamics, 59(5), 1753–1774. https://doi.org/10.1007/s00382-021-06067-2

Guo, T., Li, Y., Yong, W., Fang, P., Qin, Z., Yan, A., & Dong, Y. (2021). Non-target geographic region discrimination of Cabernet Sauvignon wine by direct analysis in real time mass spectrometry with chemometrics methods. International Journal of Mass Spectrometry, 464, 116577. https://doi.org/10.1016/j.ijms.2021.116577

Hassan, M. M., Xu, Y., Sayada, J., Zareef, M., Shoaib, M., Chen, X., Li, H., & Chen, Q. (2025). Progress of machine learning-based biosensors for the monitoring of food safety: A review. Biosensors and Bioelectronics, 267, 116782. https://doi.org/10.1016/j.bios.2024.116782

Hu, A., Yu, Z., Liu, X., Gao, W., He, Y., & Li, J. (2019). The effects of irrigation and fertilization on the migration and transformation processes of main chemical components in the soil profile. Environmental Geochemistry and Health, 41(6), 2631–2648. https://doi.org/10.1007/s10653-019-00298-3

Kamble, A., Bajaj, S., Dhaulaniya, A. S., & Balan, B. (2025). Analytical advances in food authentication and origin traceability: From mass spectrometry to AI and IoT-enabled smart sensing systems. Journal of Food Measurement and Characterization, 19, 5257–5285. https://doi.org/10.1007/s11694-025-03341-3

Kingston, K., Pratt, C., Mackay, B., Petrie, P. R., Ellis, J., & Xu, Z. (2025). The potential of integrating biochar and stable isotope technologies for regenerative viticulture under climate change. Journal of Soils and Sediments, 1–15. https://doi.org/10.1007/s11368-025-04123-6

Leder, R., Petric, I. V., Jusup, J., & Banović, M. (2021). Geographical discrimination of Croatian wines by stable isotope ratios and multielemental composition analysis. Frontiers in Nutrition, 8, 625613. https://doi.org/10.3389/fnut.2021.625613

Li, J., Qian, J., Chen, J., Ruiz-Garcia, L., Dong, C., Chen, Q., Liu, Z., Xiao, P., & Zhao, Z. (2025). Recent advances of machine learning in the geographical origin traceability of food and agro-products: A review. Comprehensive Reviews in Food Science and Food Safety, 24(1), e70082. https://doi.org/10.1111/1541-4337.70082

Li, Y., Xue, J., Cai, J., Zhang, Y., Li, F., Zha, X., & Fang, G. (2023). The spatial distribution and influencing factors of heavy metals in soil in Xinjiang, China. Sustainability, 15(23), 16379. https://doi.org/10.3390/su152316379

Miao, Y., Wang, H., Xu, X., Ye, P., Wu, H., Zhao, R., Shi, X., & Cai, F. (2022). Chemical and sensory characteristics of different red grapes grown in Xinjiang, China: Insights into wines composition. Fermentation, 8(12), 689. https://doi.org/10.3390/fermentation8120689

Mizik, T., & Balogh, J. M. (2022). The development of the Chinese wine industry and trade. International Journal of Wine Business Research, 34(4), 643–660. https://doi.org/10.1108/IJWBR-09-2021-0045

Pang, Z., Kong, Y., Froehlich, K., Huang, T., Yuan, L., Li, Z., & Wang, F. (2011). Processes affecting isotopes in precipitation of an arid region. Tellus B: Chemical and Physical Meteorology, 63(3), 352–359. https://doi.org/10.1111/j.1600-0889.2011.00532.x

Pereira, S., Baltazar, M., Branco, Z., Marques Monteiro, A. I., Serrano, A. S., Morales, A. M., Cruz, R., Casal, S., Balfagón, D., & Moura, R. (2025). Grape berries biochemical shifts from vines under summer stress treated with kaolin and silicon mixtures. Frontiers in Plant Science, 16, 1681593. https://doi.org/10.3389/fpls.2025.1681593

Pesme, J.-O. (2023). Tracing and tracking wine bottles: Protecting consumers and producers. BIO Web of Conferences, 68, 03028. https://doi.org/10.1051/bioconf/20236803028

Pilgrim, T. S., Watling, R. J., & Grice, K. (2010). Application of trace element and stable isotope signatures to determine the provenance of tea (Camellia sinensis) samples. Food Chemistry, 118(4), 921–926. https://doi.org/10.1016/j.foodchem.2008.08.077

Popîrdă, A., Luchian, C. E., Cotea, V. V., Colibaba, L. C., Scutarașu, E. C., & Toader, A. M. (2021). A review of representative methods used in wine authentication. Agriculture, 11(3), 225. https://doi.org/10.3390/agriculture11030225

Ranaweera, R. K., Capone, D. L., Bastian, S. E., Cozzolino, D., & Jeffery, D. W. (2021a). A review of wine authentication using spectroscopic approaches in combination with chemometrics. Molecules, 26(14), 4334. https://doi.org/10.3390/molecules26144334

Ranaweera, R. K., Gilmore, A. M., Capone, D. L., Bastian, S. E., & Jeffery, D. W. (2021b). Authentication of the geographical origin of Australian Cabernet Sauvignon wines using spectrofluorometric and multi-element analyses with multivariate statistical modelling. Food Chemistry, 335, 127592. https://doi.org/10.1016/j.foodchem.2020.127592

Rapa, M., Ferrante, M., Rodushkin, I., & Conti, M. E. (2024). Safety and Quality of Grapes: Elemental, Isotopic and Chemometric Analysis from Montepulciano d'Abruzzo PDO Chain. Agriculture, 14(6), 966. https://doi.org/10.3390/agriculture14060966

Rapa, M., Ferrante, M., Rodushkin, I., Paulukat, C., & Conti, M. E. (2023). Heavy metals, rare earth elements and isotopic fingerprint of Venetian Protected Designation of Origin sparkling wines. British Food Journal, 125(7), 2644–2662. https://doi.org/10.1108/BFJ-06-2022-0483

Santagostini, L., & Guglielmi, V. (2024). Geological influences on wine quality: Analyzing Nebbiolo grapes from Northern Italy. Applied Sciences, 15(1), 258. https://doi.org/10.3390/app15010258

Santesteban, L. G., Miranda, C., Barbarin, I., & Royo, J. B. (2015). Application of the measurement of the natural abundance of stable isotopes in viticulture: A review. Australian Journal of Grape and Wine Research, 21(2), 157–167. https://doi.org/10.1111/ajgw.12124

Shi, N., Zhao, Y.-F., Lu, H.-C., Tian, M.-B., Li, M.-Y., Deng, J.-Y., Wei, J.-Y., Chen, A.-S., Cheng, C.-F., & Li, S.-D. (2025). Flavoromics analysis and sensory evaluation of wines produced from nine red grape cultivars in Manas region, Xinjiang, China: Implications for terroir adaptation. Food Chemistry, 490, 145096. https://doi.org/10.1016/j.foodchem.2025.145096

Sun, X., Zhang, F., Gutiérrez-Gamboa, G., Ge, Q., Xu, P., Zhang, Q., Fang, Y., & Ma, T. (2022). Real wine or not? Protecting wine with traceability and authenticity for consumers: chemical and technical basis, technique applications, challenge, and perspectives. Critical Reviews in Food Science and Nutrition, 62(24), 6783–6808. https://doi.org/10.1080/10408398.2021.1906624

van Leeuwen, C., Barbe, J.-C., Darriet, P., Geffroy, O., Gomès, E., Guillaumie, S., Helwi, P., Laboyrie, J., Lytra, G., Le Menn, N., Marchand, S., Picard, M., Pons, A., Schüttler, A., & Thibon, C. (2020). Recent advancements in understanding the terroir effect on aromas in grapes and wines. OENO One, 54(4), 985–1006. https://doi.org/10.20870/oeno-one.2020.54.4.3983

van Leeuwen, C., Roby, J.-P., & de Rességuier, L. (2018). Soil-related terroir factors: A review. OENO One, 52(2), 173–188. https://doi.org/10.20870/oeno-one.2018.52.2.2208

Yang, C., Song, R., Ding, Y., Wang, W., & Zhang, C. (2022). Review on legal supervision system of the Chinese wine industry. Horticulturae, 8(5), 432. https://doi.org/10.3390/horticulturae8050432

Zhang, D., Zhang, Y., Lin, K., Wang, B., Shi, X., & Cheng, W. (2021). Comparison of sugars, organic acids and aroma components of five table grapes in Xinjiang. In IOP Conference Series: Earth and Environmental Science (Vol. 792, pp. 012029): IOP Publishing. https://doi.org/10.1088/1755-1315/792/1/012029